American Mineralogist, Volume 96, pages 1821–1827, 2011

Electrical conductivity of albite at high temperatures and high pressures

Haiying Hu,[1,2] Heping Li,[1,*] Lidong Dai,[1] Shuangming Shan,[1] and Chengming Zhu[1]

[1]Laboratory for Study of the Earth's Interior and Geofluids, Institute of Geochemistry, Chinese Academy of Sciences, Guiyang, Guizhou 550002, China
[2]Graduate School of Chinese Academy of Sciences, Beijing 100039, China

Abstract

The electrical conductivity of low albite has been measured using a complex impedance spectroscopic technique at 1.0–3.0 GPa and 773–1073 K in the frequency range of 10^{-1} to 10^{6} Hz in a YJ-3000t multi-anvil press. Within this frequency range, the complex impedance plane displays a semi-circular arc that represents a grain interior conduction mechanism. The electrical conductivity of albite increases with increasing temperature, and the relationship between electrical conductivity and temperature fits the Arrhenius formula. Pressure has a weak effect on the electrical conductivity of albite in the experimental pressure-temperature (*P*-*T*) range in the present work. The pre-exponential factors decrease, and the activation enthalpy increases slightly with increasing pressure. The activation energy and activation volume of albite are 0.82 ± 0.04 eV and 1.45 ± 0.28 cm^3/mol, respectively. Comparison with previous results with respect to albite indicates that our data are similar to previous data within the same temperature range. The dominant conduction mechanism in albite is suggested to be ionic conduction, where loosely bonded sodium cations, the dominant charge carriers, migrate into interstitial sites within the feldspar aluminosilicate framework. The Na diffusivity inferred from electrical conductivity of albite in this study using the Nernst-Einstein relation is consistent with that of previous studies on natural albite.

Keywords: Albite, high temperature and high pressure, electrical conductivity, conduction mechanism

Introduction

Based on the electrical conductivity of minerals measured in the laboratory at high temperatures and high pressures, researchers are eager to establish a conductivity model for complicated structural rocks that exist at various depths in the Earth's interior. The model can provide important constraints on the results of magnetotelluric (MT) and geomagnetic deep sounding (GDS), material composition, and thermal state distribution. Electrical conductivities of minerals at high temperatures and pressures are an important to explore the microstructures of materials in the Earth's interior, and are also the significant approach to relate the mineral microstructure with macroscopic properties and processes (Laštovičková 1991; Tyburczy and Fisler 1995; Gaillard 2004; Poe et al. 2008). Consequently, laboratory measurements of minerals at high *T* and *P* are the fundamental work of mineralogy, petrology, geochemistry, and geophysics.

Since quartz and feldspars comprise ~85% of the volume of the Earth's crust (Downs et al. 1996), the electrical conductivity of feldspars largely influences the crust's physical properties. Most previous studies have focused on the conductivity of quartz, gneiss, granulite, and other high-grade metamorphic rocks (Jain and Nowick 1982; Lee et al. 1983; Kronenberg and Kirby 1987; Glover and Vine 1992; Bagdassarov and Delépine 2004; Fuji-ta et al. 2004, 2007; Wang et al. 2002, 2010), whereas there has been little research on the electrical conductivity of feldspars. Albite is an end-member of the feldspars, and an understanding of the electrical conductivity of albite would be helpful to study the electrical conductivities of the entire feldspar group. Most previous experimental studies on the electrical conductivity of feldspars were carried out under atmospheric pressure and high-*T* conditions (Khitarov and Slutskii 1965; Maury 1968a, 1968b; Piwinskii and Duba 1974; Piwinskii et al. 1977; Bakhterev 2008). Recently, Ni et al. (2011) measured the electrical conductivity of synthetic anhydrous and hydrous albite glasses and liquids at 473 to 1773 K and 0.9 to 1.8 GPa in a piston-cylinder apparatus. However, the samples used were not natural crystalline feldspar. Therefore, a systemic study of the electrical conductivity of natural albite at high *T* and *P* is required.

We measured the electrical conductivity of hot-press sintered albite at temperatures from 773 to 1073 K and pressures from 1.0 to 3.0 GPa using AC impedance spectra at frequencies from 10^{-1} to 10^{6} Hz. The effect of *P* and *T* on the electrical conductivity of albite was observed, and the results obtained are compared with those of previous studies. We also discuss the conduction mechanism of albite under high *T* and *P* in detail.

* E-mail: hepingli_2007@hotmail.com

EXPERIMENTAL PROCEDURES

Sample preparation

The fresh, unaltered, massive white samples analyzed in this study are low albite obtained from a large open ore feldspar deposit in Hengshan Mountain, Hunan province, China. The samples were cleaned in acetone and ethanol before being dried in an oven. They were then ground into powder (<200 mesh) in an agate mortar and the powder was placed in a copper capsule with a 0.025 mm thick molybdenum (Mo) foil liner to prevent interdiffusion between the powdered sample and the copper tube. The inner and outer diameters of the copper capsule were 8 mm and 9.5 mm, respectively, and the height was 20 mm. To avoid anisotropy, inhomogeneity, and microcracks from affecting the electrical conductivity measurements, the albite powder sample was sintered for 1 h in a multi-anvil high-pressure apparatus at 1123 K and 1.5 GPa. The sintering conditions did not exceed the stability of albite (Downs et al. 1996). The sintered samples were then cut and polished into cylinders (6.0 mm diameter × 6.0 mm length). Contaminants on the sample surface were removed by rinsing in acetone, ethanol, and deionized water in an ultrasonic cleaner. Finally, the samples were baked in an oven at 400 K for 24 h to remove the absorbed water that might affect the complex impedance spectroscopic measurements. Electron microprobe analysis (EMPA) was performed at the State Key Lab of Ore Deposit Geochemistry, CAS, China. The chemical composition of a representative sample is presented in Table 1.

Microstructures of the hot-pressed sintered sample were observed by scanning electron microscopy (SEM), an example of which is shown in Figure 1. All grains (<100 μm in diameter) are uniform and randomly distributed. Although minor pores and microcracks are present, they are not interconnected and therefore have little to no effect on the overall electrical properties of the sample (Beekmans and Heyne 1976).

TABLE 1. Chemical composition of a sample analyzed by electronic microprobe

Oxide	wt%
SiO_2	68.54
Al_2O_3	19.40
Na_2O	11.50
K_2O	0.07
CaO	0.22
FeO	0.08
MgO	0.01
Cr_2O_3	0.11
TiO_2	0.04
BaO	0.02
Total	99.99

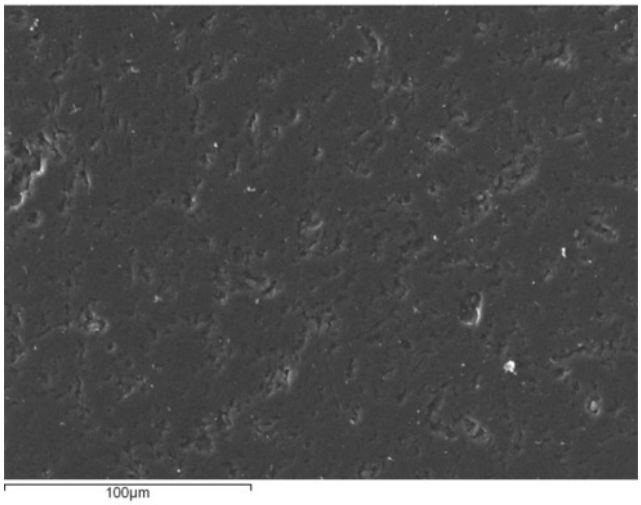

FIGURE 1. SEM image of a polycrystalline low albite sample after hot-pressing and sintering at 1123 K and 1.5 GPa for 1 h.

Experimental methods

The impedance spectroscopies of the samples were measured using the impedance/gain-phase analyzer (Solartron-1260) and multi-anvil high-*T* and high-*P* apparatus (YJ-3000t) built in the Laboratory for Study of the Earth's Interior and Geofluids, Institute of Geochemistry, CAS. Experimental procedures for the use and calibration of this instrument have been described previously (Li et al. 1999; Liu et al. 2003; Shan et al. 2007).

A schematic drawing of the high-*P* cell for electrical conductivity measurements is displayed in Figure 2. The pressure-transmitting medium was a cubic pyrophyllite (spec: 32.5 × 32.5 × 32.5 mm). To avoid the effect of pyrophyllite dehydration on the impedance spectroscopy measurement, both the pressure-transmitting medium and the end blocks were heated at 1173 K for 5 h in a muffle furnace. The heater was composed of three-layer stainless steel sheets, 0.5 mm thick, arranged around the cube. The intermediate sheet mainly consisted of aluminum oxide and boron nitride to maintain excellent insulation around the sample under high *P* and high *T*. The boron nitride was in direct contact with the sample to avoid cracking due of its softness (Fuji-ta et al. 2004). In addition, a 0.025 mm thick nickel shield connected to ground was installed between the insulating aluminum oxide and boron nitride to efficiently block external electromagnetic disturbances and to reduce temperature gradients in the sample (Xu et al. 2000b; Dai and Karato 2009). The temperature was measured using a pair of 0.5 mm diameter Pt-$PtRh_{10}$ thermocouples placed at the middle of the sample. Platinum disk electrodes (0.5 mm in thickness × 6.0 mm diameter) were placed above and below the sample. A nickel-aluminum lead was connected to each electrode.

Impedance spectra in the frequency range of 10^{-1} to 10^6 Hz were measured using a Solartron 1260 impedance/gain phase analyzer with 1 V of applied voltage. Reproducibility of the measurements (Laštovičková 1987; Nover 2005; Pommier et al. 2009) was assured by raising the pressure to the designated value at a rate of 1.5 GPa/h and the temperature to 1073 K, at which point it was held for 3 h to allow the system reach the thermal transfer equilibrium in the sample cell. Impedance spectra were measured according to the following procedure. (1) Spectra were collected every 50 K. (2) The system was stabilized for 15 min or more until reproducible data were obtained. (3) Reproducibility of data was confirmed by measuring the electrical conductivity of albite on heating and cooling at 1.0 GPa over temperatures of 773–1073 K. Then, the electrical conductivity was measured at 2.0 and 3.0 GPa as the system cooled. Temperature and pressure errors are ±10 K and ±0.1 GPa, respectively.

According to the ideal semicircles in the impedance spectra plane, an equivalent circuit composed of a resistor and capacitor in parallel was used to fit the complex impedance data in the frequency range of 10^{-1}–10^6 Hz by running the Zview program. The resistances were obtained using the same procedures at all pressures. The fitting error of the impedance spectra was less than 1.0%.

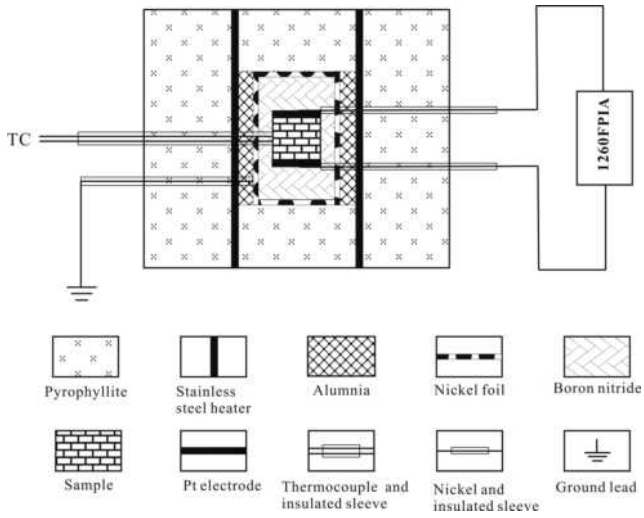

FIGURE 2. Experimental setup for electrical conductivity measurements.

Experimental results

The complex impedance, Z*, is defined by a real (resistance) and imaginary part (reactance):

$$Z^* = Z' - jZ'' \tag{1}$$

The modulus ($|Z|$) and phase angle (θ) of the complex impedance are acquired using the following equations:

$$|Z| = \sqrt{Z'^2 + Z''^2} = \frac{R}{\sqrt{1+(\omega RC)^2}} \tag{2}$$

$$tg\theta = \frac{Z''}{Z'} = \omega RC \tag{3}$$

where ω (= $2\pi f$) is the angular frequency, f is the frequency, R is the resistance, and C is the capacitance. A typical set of complex impedance data for low albite obtained at 1.0 GPa for 773 to 1073 K are shown in Figures 3 and 4. Figure 3, which is known as a Bode plot, shows the results of the modulus and phase angle of the complex impedance against frequency at different temperatures. Figure 3 shows that both the complex impedance modulus and the phase angle of the sample are strongly dependent on the temperature and frequency. The complex impedance modulus increases with decreasing frequency over the entire temperature range and reaches a constant value at about 10^3 Hz. The phase angle of the complex impedance also increases with decreasing frequency and reaches a constant value at about 10^2 Hz.

Figure 4 shows the complex impedance spectra of the samples in the form of the real part (Z') against the imaginary part (Z''). At the experimental temperatures, the complex planes show ideal semicircle arcs at frequencies of 10^{-1} to 10^6 Hz and the diameter of the semicircle arc decreases rapidly with increasing temperature. According to polycrystalline silicate studies and impedance spectra theory (Roberts and Tyburczy 1991, 1993; Huebner and Dillenburg 1995), the diameter of the semicircle arc represents the grain interior resistance of the polycrystalline low albite sample. Hence, as we described above, the resistance of the sample can be obtained from the Zview program fitting composed of RC parallel equivalent circuits. From the fitting resistance and the sample dimension, the electrical conductivity of the sample is calculated by the following equation:

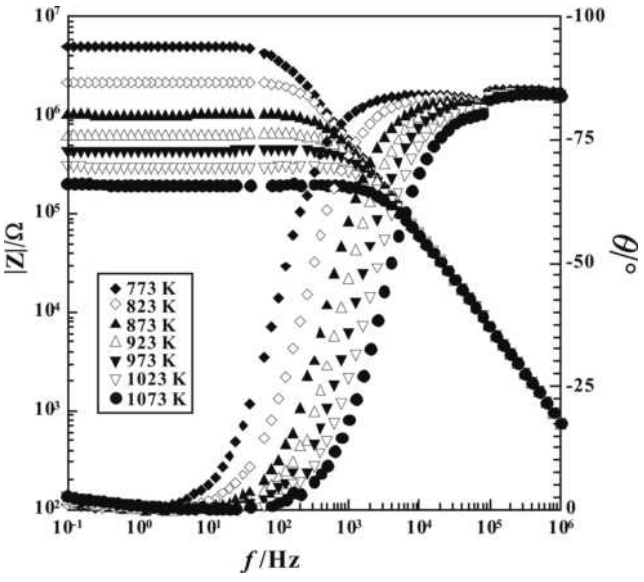

Figure 3. The modulus and phase angle of the complex impedance of polycrystalline albite against frequency at 1.0 GPa, 773–1073 K.

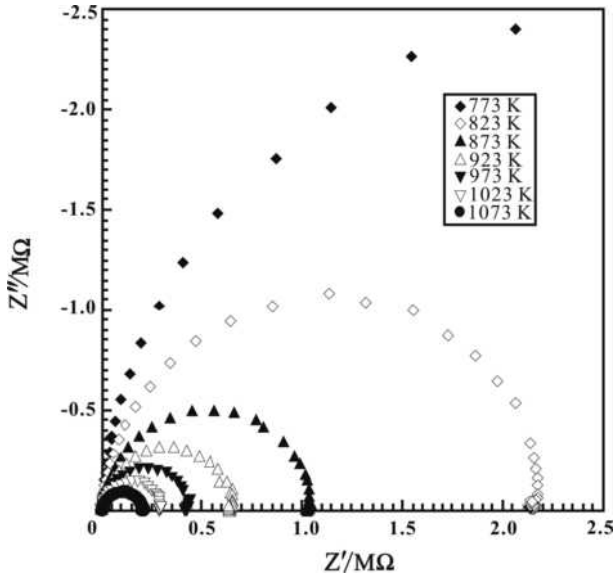

Figure 4. Z' (real component) vs. Z'' (imaginary component) plot of the complex impedance of albite at 1.0 GPa and 773 to 1073 K, with a frequency range of 0.1 Hz to 1 MHz.

$$\sigma = \frac{1}{\rho} = \frac{L}{RS} \tag{4}$$

where σ is the electrical conductivity of the sample (S/m), ρ is resistivity (Ω·m), L is the sample length (m), S is the cross-sectional area of the electrodes (m^2), and R is the resistance (Ω).

The logarithmic electrical conductivity of albite at pressures of 1.0–3.0 GPa and temperatures of 773–1073 K is plotted against the reciprocal temperature in Figure 5. Through linear fitting to the data points at the same pressure and different temperature in Figure 5, we obtained linear correlation coefficients no less than 0.9889. Therefore, the electrical conductivity of albite can be expressed using an Arrhenius formula:

$$\sigma T = A\exp(-\Delta H / kT) \tag{5}$$

where A is the pre-exponential factor (K·S/m), ΔH is the activation enthalpy (eV), which can be calculated using $\Delta H = \Delta U + P \times \Delta V$, where ΔU is the activation energy (eV), ΔV is the activation volume (cm^3/mol), P is pressure (GPa), k is the Boltzmann constant (eV/K), and T is the absolute temperature (K). These fitting parameters can be determined by plotting the slope and intercept of the logarithmic conductivity against the reciprocal temperature, the results of which are shown in Table 2. Furthermore, with these parameters we can calculate the electrical conductivity of albite at zero pressure as shown in Figure 5. The electrical conductivity of albite decreases with

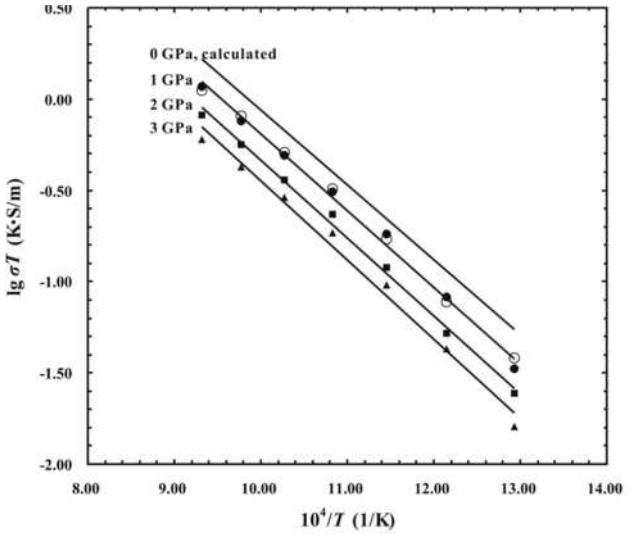

FIGURE 5. Logarithm of electrical conductivity vs. reciprocal temperature for albite at 1.0 to 3.0 GPa. The open circles represent the electrical conductivity of albite on heating at 1.0 GPa. The calculated conductivity of albite at zero pressure by using the parameters of the Arrhenius relation is also shown.

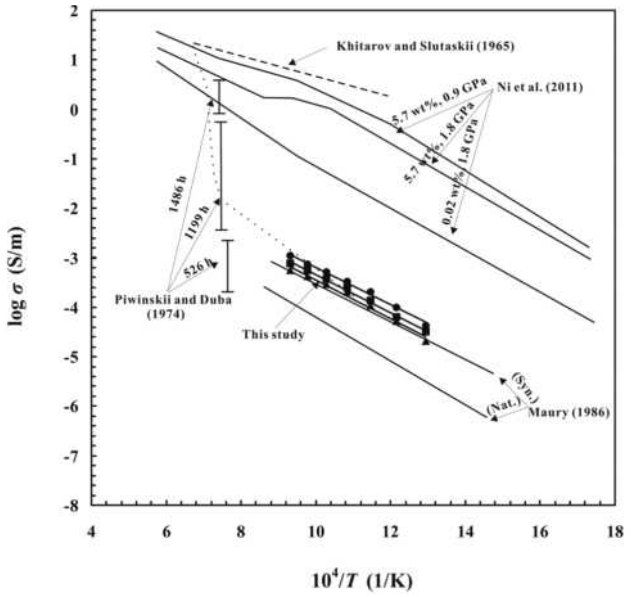

FIGURE 6. Comparison of electrical conductivity studies of albite including this study. The dotted and dashed lines indicate the electrical conductivity of powdered albite (An_3Ab_{97}) upon heating and cooling, respectively (Khitarov and Slutskii 1965). The solid lines are the results of previous studies (Maury 1968; Piwinskii and Duba 1974; Ni et al. 2011).

increasing *P* at the same temperature. For example, the electrical conductivity decreases by 0.3 log units at 1073 K from 1.0 to 3.0 GPa. Decreasing conductivity with increasing *P* reflects the increase in activation enthalpy, as shown in Table 2. In addition, the influence of pressure on the pre-exponential factor is small. As in the case of previous experiments (Xu et al. 2000b; Katsura et al. 2007), the pre-exponential factor is independent of *P* over a wide temperature range. The pre-exponential factor may be constant if extrapolations of conductivity in this study at different pressures to infinite temperature seem to converge to one value. The activation energy and activation volume are determined as 0.82 ± 0.04 eV and 1.45 ± 0.28 cm^3/mol, respectively.

DISCUSSION

Comparison with previous studies

The conductivity data obtained in this study are compared with previous measurements on albite (Figure 6 and Table 3). Khitarov and Slutskii (1965) measured the electrical conductivity of powdered albite (An_3Ab_{97}) upon heating (dotted lines) and cooling (dashed lines) at 0.28 GPa and attributed the large change in conductivity due to the melting of albite. Our experimental results agree well with those of Khitarov and Slutskii (1965) on heating at the same temperature. Although the activation energy in the work of Khitarov and Slutskii (1965) cannot be obtained, the slope of the logarithmic conductivity against the reciprocal temperature on heating is similar to that of ours. Hence, the activation energy should be consistent with our results. Maury (1968a, 1968b) performed electrical conductivity measurements on synthetic and natural albite at 673 to 1173 K and ambient pressure in the frequency range of 1–10 kHz using an AC impedance spectroscopy method. Our results are generally in agreement with those of the synthetic sample but are significantly higher than those of the natural sample measured by Maury (1968a, 1968b) over a similar temperature range. This discrepancy may be attributed to anisotropy and microcracks in the natural albite used by Maury (1968a, 1968b). Although the relationship between electrical conductivity and anisotropy of albite is unclear, research on the anisotropy of the electrical conductivity of single crystals of olivine, quartz, and diopside indicate that the electrical conductivity of minerals is significantly different along different crystallographic directions (Cygan and Lasaga 1986; Schock et al. 1989; Dai et al. 2005; Poe et al. 2010; Wang et al. 2010). In addition, a diffusion experiment of alkali feldspars has also shown that the alkali diffusion rates vary in different crystallographic directions (Christoffersen et al. 1983). According to the data of Christoffersen et al. (1983), alkali inter-diffusion is about 10 times faster normal to [001] than it is normal to [010], and the rate is intermediate parallel to [100] and [011]. Therefore, this suggests that the electrical conductivity of feldspars is also anisotropic. Because our samples were made of hot-pressed sintered natural albite aggregates, in which albite grains are randomly distributed, and measured at higher pressures, it is very likely that we have eliminated the effect of anisotropy and microcracks on the electrical conductivity. The synthetic albite

TABLE 2. Fitted parameters of the Arrhenius relation for the electrical conductivity of albite

Run no.	*P* (GPa)	*T* (K)	Log *A*	*A* (K·S/m)	Δ*H* (eV)	R^2	Δ*U* (eV)	Δ*V* (cm^3/mol)
N100	1.0	773–1073	4.00 ± 0.15	10000	0.84 ± 0.03	0.9951	0.82 ± 0.04	1.45 ± 0.28
N105	2.0	773–1073	3.92 ± 0.14	8317	0.85 ± 0.03	0.9956		
N109	3.0	773–1073	3.89 ± 0.23	7762	0.87 ± 0.04	0.9889		

TABLE 3. Summary of samples, experimental conditions, and results of electrical conductivity measurements of albite by various studies

Sample	*P* (GPa)	*T* (K)	Methods of measurement	$Log_{10}\ \sigma_0$ (S/m)	ΔU (eV)	References
Low albite	1.0–3.0	773–1073	AC impedance spectroscopy	3.94 ± 0.21	0.82 ± 0.04	This study
Albite glasses	1.8	573–1073	AC Impedance spectroscopy	3.18	0.84 ± 0.01	Ni et al. (2011)
		1073–1773		3.87	0.98 ± 0.05	
Amelia albite	Ambient pressure	1353, 1373,1384	DC	–	–	Piwinskii and Duba (1974)
Natural albite	Ambient pressure	673–1173	AC Impedance spectroscopy	0.15	0.86	Maury (1968)
Synthetic albite		673–1173		0.08	0.72	
Albite (An_3Ab_{97})	0.28	<1573	DC	–	–	Khitarov and Slutskii (1965)

of Maury (1968a, 1968b) is similar to our sample. Piwinskii and Duba (1974) measured the single-crystal Amelia albite at room pressure by a DC method. Comparison with these data are difficult because the electrical conductivity of the Amelia albite was conducted as a function of time at 1353, 1373, and 1384 K at 1.6 kHz. These conditions are rather different from our experimental conditions. Ni et al. (2011) measured the electrical conductivity of albite glasses and liquids, both hydrous and anhydrous, at 473 to 1773 K and 0.9 to 1.8 GPa using an impedance spectroscopic method in a piston-cylinder apparatus. Their results were much higher than those obtained in the present study. The large difference between these two studies was attributed to the presence of water, which facilitates Na transport discussed in detail by Ni et al. (2011). Because the samples used in this study were entirely dry, it is, therefore, understandable that the absolute conductivity values of our sample are much lower than those of Ni et al. (2011). It seems that a small amount of water can raise the electrical conductivity by many orders of magnitude.

Conduction mechanism

Under the experimental conditions, the linear relationship between the logarithmic conductivity and the reciprocal temperature suggests that there is only one transport mechanism for the electrical conductivity of our samples. According to studies of the electrical conductivity of feldspars and other aluminosilicate minerals (Ni et al. 2011; Jones et al. 2010), the conduction mechanism of albite is suggested to be ionic conduction at high *T* and *P*. The charge carriers are sodium ions, which migrate into interstitial sites in the albite aluminosilicate framework. The micromechanism of ion conduction in solid material is the diffusion of charge carriers, and the relationship between the electrical conductivity and diffusion can be expressed by the Nernst-Einstein equation (Chakraborty 1995):

$$\sigma = Dcq^2 / H_r kT \quad (6)$$

where H_r is the Haven ratio related to the correlation factor, which usually has a value between 0.1 and 1.0, *D* is the diffusivity, *c* is the concentration, *q* is the electrical charge of the charged species, *k* is the Boltzmann constant, and *T* is the temperature in Kelvin. The conduction mechanism of olivine, quartz, and other minerals, deduced by the Nernst-Einstein relation, has been extensively discussed (Verhoogen 1952; Kronenberg and Kirby 1987; Constable and Duba 2002). Therefore, it is a valid method to determine the major charge carrier in minerals and rocks. The results of cation diffusion experiments in feldspars at high *T* have indicated that Na^+, with its small diameter and smaller charge, diffuses by means of an interstitial mechanism, whereas K^+, Ca^{2+}, and Sr^{2+} diffuse by means of a vacancy mechanism (Lin and Yund 1972; Behrens et al. 1990; Giletti and Casserly 1994; Giletti and Shanahan 1997). In addition, Lin and Yund (1972) performed sodium self-diffusion measurements of low albite at 473 to 873 K using tracer element methods and obtained an activation energy of 0.82 eV. Their result is similar to ours. Hence, we can conclude that electrical conduction in albite occurs by means of a similar diffusion process at high *T* and *P*.

The Arrhenius parameters of albite are displayed in Table 2. The determined activation energy and activation volume are 0.82 ± 0.04 eV and 1.45 ± 0.28 cm^3/mol, respectively. According to the positive activation volume of albite at high *T* and the characteristic ionic conduction mechanism in which there is usually a positive volume (Aboagye and Friauf 1975; Samara 1984), the conduction mechanism of albite is also suggested to be the interstitial migration mechanism of sodium cations under our experimental *T* and *P* conditions. The point defect in the albite crystal is the Frenkel defect (Behrens et al. 1990), and the defect reaction can be written as follow:

$$Na^{X}_{A_1} = Na^{\bullet}_{i} + \square'_{A_1} \quad (7)$$

where $Na^{X}_{A_1}$ is a sodium ion in a normal lattice site (A_1 sites), $Na^{\bullet}_{i}$ is a sodium ion occupying the interstitial site, and $\square_{A_1}$ is the vacancy of sodium ion in its normal lattice site of A_1. At high *T*, the Na ions in the A_1 site gain enough energy to cross an energy barrier and reach an adjacent interstitial position (a normally unoccupied lattice position), leaving behind a sodium site vacancy. In the present experiment, the crystal lattice of albite is compressed due to increasing *P*, and the charge carriers need more energy to cross the energy barrier. This reflects the fact that the activation energy increases with increasing pressure. Therefore, a decrease in the amount of charge carrier due to the suppression of interstitial ions by pressure results in a decrease in electrical conductivity (Jones 2004; Li et al. 1993).

In addition, the activation energy (0.82 ± 0.04 eV) of albite obtained in this study is slightly larger than the 0.72 eV for synthetic albite, but in general agreement with the 0.86 eV for natural albite given by Maury (1968a, 1968b). Furthermore, it is also consistent with an activation energy of 0.85 eV for anhydrous albite glasses in the temperature range of 573 to 1073 K obtained by Ni et al. (2011), who suggested that the dominating conduction mechanism is the motion of sodium cations. Jones et al. (2010) obtained activation energies of 0.74 to 0.97 eV by measuring the electrical conductivity of natural leucite at 623 to 1073 K and 2.5 to 6.0 GPa, and identified an ionic conduction mechanism in which potassium cations migrate within channels in the leucite framework. Our activation energy is in the range of that of Jones et al. (2010), and it is reasonable to propose that leucite and albite have similar conduction mechanisms because of their similar aluminosilicate frameworks.

Implications

The conductivity data obtained in this study can provide a reference for magnetotelluric studies in regions that are dominated by granite and pegmatite, which are mainly composed of feldspar and quartz. Moreover, laboratory data of minerals at high T and high P can provide a reproducible and reliable database for establishing the electrical conductivity models of rocks in the Earth's interior (Nover 2005), which is essential for the inversion of field magnetotelluric (MT) and geomagnetic depth sounding (GDS) results. In the Earth's crust, feldspars with lower electrical conductivity can be regarded as insulators in a rock matrix when compared to other rock-forming minerals, and therefore, the electrical conductivity of rocks may decrease with the increasing content of albite under dry conditions. Xu et al. (2000a) successfully used mixing relationships to establish the conductivities of multiphase materials in the Earth's mantle. They yielded mineral physics-based conductivity-depth models for the upper mantle and the transition zone that agree well with field geomagnetic models. Consequently, laboratory data can provide an important constraint for interpreting MT results.

If only one type of ion contributes to the conductivity in ion-conducting material, the Nernst-Einstein equation permits one to define a conductivity diffusion coefficient D_σ that is calculated by Equation 6, assuming that H_r is equal to 1. Using the concentration of Na cations (in molar/cm^3), Na^+ diffusivities can be calculated at 1.0–3.0 GPa through the electrical conductivity data in this study and compared with previous studies for albite. The results are shown in Figure 7. The calculated Na diffusivities in this study are very consistent with Na self-diffusivities of natural albite measured by Sippel (1963) and also agree with those of the pure low-albite at the same temperature measured by Lin and Yund (1972). However, the result measured by Kasper (1975) at 200 MPa water pressure using an isotopic method is obviously higher than that of ours, which can be attributed to the different experimental conditions and method. We note that D_σ has the dimensions of a diffusion coefficient (D*), which can be measured using Fick's law (Voss et al. 2004). The ratio D*/$D_\sigma = H_r$, which is usually equal to or less than unity, can provide valuable information about the diffusion mechanism (Jain et al. 1983). In addition, Heuer et al. (2002) showed that the inverse of the Haven ratio can be regarded as a measure for the degree of collectivity in ionic motion by performing molecular-dynamics simulations on the Li motion in lithium silicate glasses.

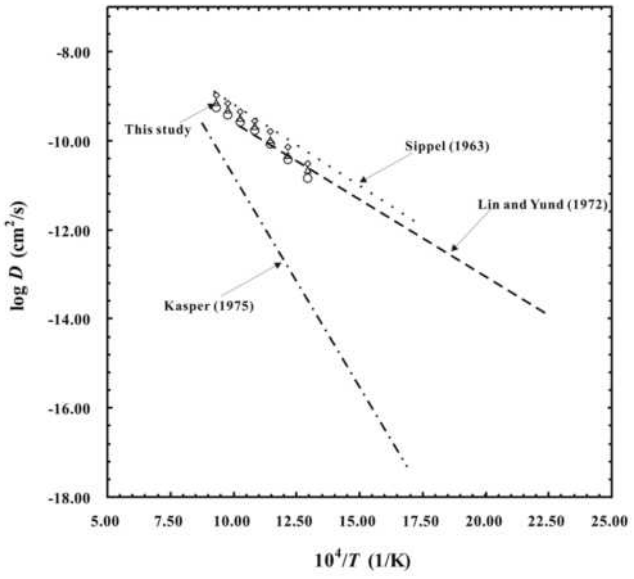

FIGURE 7. The inferred diffusivities using the Nernst-Einstein relation are shown at 1.0 GPa (open diamonds), 2.0 GPa (open triangles), 3.0 GPa (open circles). The dotted line is sodium self-diffusion data for a natural albite from Sippel (1963). The dashed line indicates the self-diffusion of Na^{22} in a pure low albite from Lin and Yund (1972). The dot-dashed line shows the Na^+ diffusion in low albite from Kasper (1975).

The study on the relationship between the electrical conductivity of minerals and diffusion coefficient has been extensively developed by material scientists but not by many geologists. It is very useful to develop such research in minerals to offer geochemists valuable information about element diffusion mechanisms (Behrens et al. 1990; Gaillard 2004). On the other hand, the electrical conductivities of minerals have also been successfully calculated from diffusion coefficient data using the Nernst-Einstein equation for the purpose of inferring the conduction mechanism and comparison with MT data (Verhoogen 1952; Kronenberg and Kirby 1987; Hier-Majumder et al. 2005; Hae et al. 2006). However, there is a dearth of research on the diffusion of minerals by electrical conductivity data. Consequently, the diffusion coefficient calculated using electrical conductivity data for albite can provide an important constraint on sodium self-diffusion in albite. More theoretical and experimental studies are required.

ACKNOWLEDGMENTS

This research was financially supported by the Knowledge-Innovation Key Orientation Project of CAS (Grant Nos. KZCX2-YW-Q08-3-4 and KZCX2-YW-QN110) and NSF of China (Grant Nos. 40974051 and 41174079).

REFERENCES CITED

Aboagye, J. and Friauf, R. (1975) Anomalous high-temperature ionic conductivity in the silver halides. Physical Review B, 11, 1654–1664.

Bagdassarov, N.S. and Delépine, N. (2004) α-β inversion in quartz from low frequency electrical impedance spectroscopy. Journal of Physics and Chemistry of Solids, 65, 1517–1526.

Bakhterev, V.V. (2008) High-temperature electric conductivity of some feldspars. Doklady Earth Sciences, 420, 554–557.

Beekmans, N. and Heyne, L. (1976) Correlation between impedance, microstructure and composition of calcia-stabilized zirconia. Electrochimica Acta, 21, 303–310.

Behrens, H., Johannes, W., and Schmalzried, H. (1990) On the mechanisms of cation diffusion processes in ternary feldspars. Physics and Chemistry of Minerals, 17, 62–78.

Chakraborty, S. (1995) Diffusion in silicate melts. In J.F. Stebbins, P.F. McMillan, and D.B. Dingwell, Eds., Structure, Dynamics, and Properties of Silicate Melts, 32, p. 411–503. Reviews in Mineralogy and Geochemistry, Mineralogical Society of America, Chantilly, Virginia.

Christoffersen, R., Yund, R.A., and Tullis, J. (1983) Inter-diffusion of K and Na in alkali feldspars: diffusion couple experiments. American Mineralogist, 68, 1126–1133.

Constable, S. and Duba, A. (2002) Diffusion and mobility of electrically conducting defects in olivine. Physics and Chemistry of Minerals, 29, 446–454.

Cygan, R.T. and Lasaga, A.C. (1986) Dielectric and polarization behavior of forsterite at elevated temperatures. American Mineralogist, 71, 758–766.

Dai, L.D. and Karato, S. (2009) Electrical conductivity of wadsleyite at high temperatures and high pressures. Earth and Planetary Science Letters, 287, 277–283.

Dai, L.D., Li, H.P., Liu, C.Q., Su, G.L., and Cui, T.D. (2005) In situ control of oxygen fugacity experimental study on the crystallographic anisotropy of the electrical conductivities of diopside at high temperature and high pressure. Acta Petrologica Sinica, 21, 1737–1742.

Downs, R., Andalman, A., and Hudacsko, M. (1996) The coordination numbers of

Na and K atoms in low albite and microcline as determined from a procrystal electron-density distribution. American Mineralogist, 81, 1344–1349.
Fuji-ta, K., Katsura, T., and Tainosho, Y. (2004) Electrical conductivity measurement of granulite under mid- to lower crustal pressure-temperature conditions. Geophysical Journal International, 157, 79–86.
Fuji-ta, K., Katsura, T., Matsuzaki, T., Ichik, M., and Kobayashi, T. (2007) Electrical conductivity measurement of gneiss under mid- to lower crustal P-T conditions. Tectonophysics, 434, 93–101.
Gaillard, F. (2004) Laboratory measurements of electrical conductivity of hydrous and dry silicic melts under pressure. Earth and Planetary Science Letters, 218, 215–228.
Giletti, B.J. and Casserly, J.E.D. (1994) Strontium diffusion kinetics in plagioclase feldspars. Geochimica et Cosmochimica Acta, 58, 3785–3793.
Giletti, B.J. and Shanahan, T.M. (1997) Alkali diffusion in plagioclase feldspar. Chemical Geology, 139, 3–20.
Glover, P. and Vine, F. (1992) Electrical conductivity of carbon-bearing granulite at raised temperatures and pressures. Nature, 360, 723–726.
Hae, R., Ohtani, E., Kubo, T., Koyama, T., and Utada, H. (2006) Hydrogen diffusivity in wadsleyite and water distribution in the mantle transition zone. Earth and Planetary Science Letters, 243, 141–148.
Heuer, A., Kunow, M., Vogel, M., and Banhatti, R. (2002) Characterization of the complex ion dynamics in lithium silicate glasses via computer simulations. Physical Chemistry Chemical Physics, 4, 3185–3192.
Hier-Majumder, S., Anderson, I.M., and Kohlstedt, D.L. (2005) Influence of protons on Fe-Mg interdiffusion in olivine. Journal of Geophysical Research, 110, B02202, DOI: 10.1029/2004JB003292.
Huebner, J.S. and Dillenburg, R.G. (1995) Impedance spectra of hot, dry silicate minerals and rock: qualitative interpretation of spectra. American Mineralogist, 80, 46–64.
Jain, H. and Nowick, A.S. (1982) Electrical conductivity of synthetic and natural quartz cystals. Journal of Applied Physics, 53, 477–481.
Jain, H., Peterson, N., and Downing, H. (1983) Tracer diffusion and electrical conductivity in sodium-cesium silicate glasses. Journal of Non-Crystalline Solids, 55, 283–300.
Jones, A. (2004) Alkali ion migration in albite and K-feldspar. Physics and Chemistry of Minerals, 31, 313–320.
Jones, R.L., Thrall, M., and Henderson, C.M.B. (2010) Complex impedance spectroscopy and ionic transport properties of natural leucite, $K_{0.90}Na_{0.08}[Al_{0.98}Si_{2.02}]O_6$, as a function of temperature and pressure. Mineralogical Magazine, 74, 507–519.
Kasper, R.B. (1975) Cation and oxygen diffusion in albite, p. 143. Ph.D. thesis, Brown University, Providence, Rhode Island.
Katsura, T., Yokoshi, S., Kawabe, K., Shatskiy, A., Okube, M., Fukui, H., Ito, E., Nozawa, A., and Funakoshi, K.-i. (2007) Pressure dependence of electrical conductivity of (Mg, Fe) SiO3 ilmenite. Physics and Chemistry of Minerals, 34, 249–255.
Khitarov, N. and Slutskii, A. (1965) The effect of pressure on the melting temperatures of albite and basalt based on electrocondcutivity measurements. Geokhimiy, 12, 1395–1403.
Kronenberg, A.K. and Kirby, S.H. (1987) DC time dependence and transition in charge carriers. American Mineralogist, 72, 739–747.
Laštovičková, M. (1987) Electrical conductivity of some minerals at high temperature and for extended times. Physics of the Earth and Planetary Interiors, 45, 204–208.
——— (1991) A review of laboratory measurements of the electrical conductivity of rocks and minerals. Physics of the Earth and Planetary Interiors, 66, 1–11.
Lee, C., Vine, F., and Ross, R. (1983) Electrical conductivity models for the continental crust based on laboratory measurements on high-grade metamorphic rocks. Geophysical Journal of the Royal Astronomical Society, 72, 353–371.
Li, H.P., Xie, H.S., Guo, J., Zhang, Y.M., and Xu, Z.M. (1999) In situ control of oxygen fugacity at high temperature and high pressure. Journal of Geophysical Research, 104, 439–451.
Li, X., Ming, L.C., and Manghnani, M.H. (1993) Pressure dependence of the electrical conductivity of perovskite. Journal of Geophysical Research, 98, 501–508.
Lin, T.H. and Yund, R.A. (1972) Potassium and sodium self-diffusion in alkali feldspar. Contributions to Mineralogy and Petrology, 34, 177–184.
Liu, W., Du, J., Yong, Y., Bai, P., and Wang, C. (2003) Correction of temperature gradient in sample cell of pulse transmission experimental setup on multi-anvil high pressure apparatus. Chinese Journal of High Pressure Physics, 17, 95–100.
Maury, R. (1968a) Conductibilite electrique des tectosilicates. I. Methode et resultats experimentaux. Bulletin de la Societe Francaise de Mineralogie et Cristallographie, 91, 267–278.
——— (1968b) Conductivilite electrique des tectosilicates. II. Discussion des resultants. Bulletin de la Societe Francaise de Mineralogie et Cristallographie, 91, 355–366.
Ni, H., Keppler, H., Manthilake, M., and Katsura, T. (2011) Electrical conductivity of dry and hydrous $NaAlSi_3O_8$ glasses and liquids at high pressures. Contributions to Mineralogy and Petrology, 162, 501–513.
Nover, G. (2005) Electrical properties of crustal and mantle rocks—a review of laboratory measurements and their explanation. Surveys in Geophysics, 26, 593–651.
Piwinskii, A.J. and Duba, A.G. (1974) High temperature eletrical conductivity of albite. Geophysical Research Letters, 1, 209–211.
Piwinskii, A.J., Duba, A.G., and Ho, P. (1977) The electrical conductivity of low and high albite throughout its melting interval at 100KPa. Canadian Mineralogist, 15, 196–197.
Poe, B.T., Romano, C., Varchi, V., Misiti, V., and Scarlato, P. (2008) Electrical conductivity of a phonotephrite from Mt. Vesuvius: The importance of chemical composition on the electrical conductivity of silicate melts. Chemical Geology, 256, 192–201.
Poe, B., Romano, C., Nestola, F., and Smyth, J. (2010) Electrical conductivity anisotropy of dry and hydrous olivine at 8 GPa. Physics of the Earth and Planetary Interiors, 181, 103–111.
Pommier, A., Gaillard, F., and Pichavant, M. (2009) Time-dependent changes of the electrical conductivity of basaltic melts with redox state. Geochimica et Cosmochimica Acta, 74, 1653–1671.
Roberts, J.J. and Tyburczy, J.A. (1991) Frequency dependent electrical properties of polycrystalline olivine compacts. Journal of Geophysical Research, 96, 16205–16222.
——— (1993) Impedance spectroscopy of single and polycrystalline olivine: evidence for grain boundary transport. Physics and Chemistry of Minerals, 20, 19–26.
Samara, G.A. (1984) High-pressure studies of ionic conductivity in solids. Solid State Physics, 38, 1–80.
Schock, R.N., Duba, A.G., and Shankland, T.J. (1989) Electrical conduction in olivine. Journal of Geophysical Research, 94, 5829–5839.
Shan, S.M., Wang, R.P., Guo, J., and Li, H.P. (2007) Pressure calibration for the sample cell of YJ-3000t multi-anvil press at high temperature and high pressure. Chinese Journal of High Pressure Physics, 21, 367–372.
Sippel, R. (1963) Sodium self diffusion in natural minerals. Geochimica et Cosmochimica Acta, 27, 107–120.
Tyburczy, J.A. and Fisler, D.K. (1995) Electrical properties of minerals and melts. Mineral Physics and Crystallography, AGU Reference, 185–208.
Verhoogen, J. (1952) Ionic diffusion and electrical conductivity in quartz. American Mineralogist, 37, 637–655.
Voss, S., Imre, A., and Mehrer, H. (2004) Mixed-alkali effect in Na-Rb borate glasses: A tracer diffusion and electrical conductivity study. Physical Chemistry Chemical Physics, 6, 3669–3675.
Wang, D.J., Li, H.P., Liu, C.Q., Yi, L., Ding, D.Y., Su, G.L., and Zhang, W.G. (2002) Electrical conductivity of synthetic quartz crystals at high temperature and pressure from complex impedance measurements. Chinese Physics Letters, 19, 1211–1213.
Wang, D.J., Li, H.P., Yi, L., Matsuzaki, T., and Yoshino, T. (2010) Anisotropy of synthetic quartz electrical conductivity at high pressure and temperature. Journal of Geophysical Research, 115, B09211, DOI: 10.1029/2009JB006695.
Xu, Y.S., Shankland, T.J., and Poe, B.T. (2000a) Laboratory-based electrical conductivity in the earth's mantle. Journal of Geophysical Research, 105, 27865–27875.
Xu, Y.S., Shankland, T.J., and Duba, A.G. (2000b) Pressure effect on electrical conductivity of mantle olivine. Physics of the Earth and Planetary Interiors, 118, 149–161.

MANUSCRIPT RECEIVED JANUARY 28, 2011
MANUSCRIPT ACCEPTED JULY 15, 2011
MANUSCRIPT HANDLED BY SIMON REDFERN